

## INFLUENCE OF POLYCHEMOTHERAPY ON THE MORPHOLOGY OF METASTASES AND KIDNEY OF RESISTANT RLS-BEARING MICE

E.V. Zonov<sup>1,2</sup>, E.I. Voronina<sup>3</sup>, M.A. Zenkova<sup>1</sup>, T.A. Ageeva<sup>3</sup>, E.I. Ryabchikova<sup>1,\*</sup>

<sup>1</sup>*Institute of Chemical Biology and Fundamental Medicine, Siberian Branch of Russian Academy of Sciences, Novosibirsk 630090, Russia*

<sup>2</sup>*Novosibirsk State University, Novosibirsk 630090, Russia*

<sup>3</sup>*Novosibirsk State Medical University, Novosibirsk 630091, Russia*

**Aim:** Polychemotherapy (PCT), widely used for the antitumor treatment has a pronounced toxic effect on the organism, and its cytostatic effect sometimes is canceled by multidrug resistance of a neoplasia. Comprehension of the nature and development of pathological changes caused by the PCT during the treatment of cancer is very important to improve the efficiency of the therapy and to clarify the mechanisms of tumor-host interactions. This study was aimed to examine PCT impact on kidney cells and tissues in mice with transplanted resistant lymphosarcoma (RLS) and to analyze morphology of metastases of the tumor in kidney during PCT. **Materials and Methods:** Male mice CBA/LacSto (55 animals) were intramuscularly implanted in the right hind paw by  $10^5$  cells/ml of tumor RLS (a diffuse large B-cell lymphosarcoma) with multi-drug resistance (MDR) phenotype. Mice received combination of cyclophosphamide (50 mg/kg), oncovin (0.1 mg/kg), hydroxydaunorubicin (4 mg/kg), and prednisone (5 mg/kg) accordingly to CHOP scheme each 7 days after inoculation of the tumor. The kidneys were sampled on days 1, 3 and 7 after each series of injection of PCT preparations and processed for light and electron microscopy, immunohistochemical analysis of Ki-67 and Apaf-1 proteins also was performed. **Results:** Tumor RLS produced metastases comprised of small cells in the kidneys of mice after 8 days post inoculation. Application of PCT resulted in destruction of small-cell metastases and development of many large-cell metastases in kidney. Application of PCT induced the development of prominent damage of nephron cells, primarily in S3 segments of proximal tubules. Even one series of PCT caused reduction of basal plasma folds in these cells and alteration of mitochondria. Damage of proximal tubules and involvement of distal tubules, renal bodies and interstitial tissue in the pathologic process, increased during the experiment. This work presents the description of morphological changes in kidney as well as of the tumor metastases under PCT influence. **Conclusion:** The obtained data should be considered while designing of remedies for recovery of internal organs functions after antitumor PCT.

**Key Words:** MDR-phenotype lymphosarcoma, mice, metastasis, kidney, polychemotherapy.

Polychemotherapy (PCT) is one of the main modalities for treatment of human tumors, however high toxicity limits its application [1, 2]. Kidneys and liver, which are responsible for detoxification of the organism, are most affected by PCT [3, 4], and need special treatment to improve their functions. The development of pathological changes in these organs during PCT was not examined; in publications we can see just recorded facts of pathological changes in organs at the moment of patient's death [5, 6]. Meantime, knowledge what is the nature of pathological changes caused by PCT and how they progress during the courses of PCT is very important for understanding of their mechanisms. It is necessary to trace the effect of repeated injections of PCT preparations on the visceral organs in the dynamics of disease. Studies of this kind could be performed in appropriate animal experimental models. One of such models is diffuse large-B-cell lymphosarcoma called "resistant lymphosarcoma" (RLS) in CBA mice. The tumor has multi-drug resistance (MDR) phenotype, which is due to overexpression of genes *mdr1b* and *bcl-2*, reduced expression of gene *p53* and also to low concentration of ceramide in tumor cells. These features

provide "evacuation" of drugs out of the cell and also impede initiation of apoptosis in tumor RLS [7, 8]. Such type of MDR is observed also in humans [9, 10], what makes this experimental model particularly valuable.

Goal of our study was to examine PCT impact on kidneys of mice inoculated with tumor RLS and to analyze morphology of metastases of the tumor in this organ during PCT treatment. We used CHOP chemotherapy scheme (cyclophosphamide, hydroxydaunorubicin, oncovin, prednisone), which is widely used in clinic of lymphomas [2]. We tried to be as close as possible to way of human treatment and applied the same timing and doses of the preparations at mice inoculated with tumor RLS.

### MATERIALS AND METHODS

**Mice.** Male mice of CBA/LacSto line (further CBA) weighing 22–25 g were kept under natural lighting in cages (10 animals in each) and had free access to commercial food and water. Housing and care of the animals, as well as the experiments, corresponded to article 11 of Helsinki declaration of second Medical Association (1964), "International guidelines for conducting biomedical researches using animals" (1985) and "Rules of laboratory practice in Russian Federation" (Order of Department of Health № 267, 19.06.2003).

**Tumor.** RLS is a diffuse large B-cell lymphosarcoma, which was obtained in Institute of Cytology and Genetics of SB RAS and maintained in ascities form [11]. The tumor

Received: December 19, 2012.

\*Correspondence: Fax: +7 383 363 51 53

E-mail: lenryab@yandex.ru

**Abbreviations used:** CHOP – cyclophosphamide, hydroxydaunorubicin, oncovin, prednisone; MDR – multi-drug resistance; PCT – polychemotherapy; RLS – resistant lymphosarcoma.

RLS possesses MDR phenotype and is cross-resistant to cytostatic preparations such as adriablastin, vinblastin, doxorubicin and citarabin [7]. We applied experimental protocol of lymphosarcoma modeling in mice developed earlier [4]. Briefly, tumor cells in ascities fluid were washed by saline and diluted with saline to concentration  $10^5$  cells/ml. Mice (55 animals) received 0.2 ml of cell suspension by intramuscular injection in the right hind paw.

**Drugs.** Cyclophosphamide (Mediafarm, Russia), Hydroxydaunorubicin (Mediafarm, Russia), Oncovin (Lens-Farm, Russia) and Prednisone (Ferain, Russia) were dissolved in sterile saline and injected at doses of 50; 4; 0.1 and 5 mg/kg, respectively. The same concentrations are used in humans receiving PCT of lymphosarcomas under the scheme CHOP [4].

**Experimental model.** Mice received standard combination of PCT preparations under the scheme CHOP each 7 days after inoculation of the tumor: cyclophosphamide, oncovin and prednisone were injected intraperitoneally at intervals of 20–25 min. The volume of each injection was 0.2 or 0.25 ml. The hydroxydaunorubicin was injected into tail vein in a volume of 0.1 ml. Mice were sacrificed by cervical dislocation, cavities were opened and visceral organs visually examined. The kidneys were collected from experimental animals after 1, 3 and 7 days after each injection of PCT preparations. Kidneys were cut into two halves along the long axis and placed into 4% paraphormaldehyde in Hank's balanced solution for 24–48 h. Five intact mice also were used to obtain "normal" kidneys for morphological study.

**Histopathological and immunohistochemical studies.** The samples for light microscopy were routinely processed using Zeiss STP 120–1 (Zeiss, Germany) machine and embedded in paraffin. Sagittal sections (3–4  $\mu$ m) of the whole kidney were prepared and routinely stained with hematoxylin and eosin. Paraffin sections for immunohistochemical analysis were mounted on polylysine-coated slides (Thermo Scientific, USA). Reactions with antibodies to proteins Ki-67 and Apaf-1 were performed according to manufacturer's protocols (Abcam, Great Britain). Protein Ki-67 is a nuclear protein and serves as a marker of proliferating cells. The protein reveals itself in late G1-phase, S-, G2- and M-phases of cell cycle and is absent in cells, which are in G0-phase. The protein is located in perinuclear region, in cell nucleus, and also on chromosomes' surface [12, 13]. Protein Apaf-1 (apoptotic peptidase activation factor 1) is an apoptosis marker and is located in cytosol. Apaf-1 is activated by cytochrome-c and takes a part in formation of apoptosome and in activation of caspase-9 [14]. Reaction product was visualized by detection system (Novocastra, Great Britain) and AEC chromogen (Sigma, USA), staining of sections was finished with Erlich's hematoxylin. Immunohistochemical analysis of kidneys of mice received the treatment was carried out on 1<sup>st</sup> and 7<sup>th</sup> days after each injection of the preparations.

Paraffin sections were examined in light microscopes Zeiss Axioscope 40 with digital camera AxioCam MRc (Zeiss, Germany) and Leica DM 2500 with digital camera Leica DFC420 C (Leica, Germany).

**Electron microscopy.** Fixed kidneys were sliced into 1–2 mm thick strips, and postfixed in 1% osmium tetroxide solution, routinely processed and embedded into a mixture of epon-araldite (SPI, USA). The same protocol was applied for processing of tumor RLS cells from ascities fluid which was used for the tumor inoculation. Semithin sections were prepared from hard blocks and stained with Azur 2. The sections were examined in light microscope and areas for ultrathin sectioning were selected. Ultrathin and semithin sections were cut on ultramicrotome Ultracut-6 (Reichert-Young, Austria), routinely contrasted by uranylacetate and lead citrate (SPI, USA), and examined in transmission electron microscope JEM 1400 (Jeol, Japan). The images were collected by side-mounted digital camera Veleta (SIS, Germany).

## RESULTS AND DISCUSSION

RLS tumor cells of ascitic fluid that was used for the inoculation of mice have been examined by means of electron microscopy. Cell population mainly comprised of small cells having diameter of 4–6  $\mu$ m. Remaining cells varied in size and reached 15  $\mu$ m in diameter. Both small and large cells had roundish shape and rare short protrusions on the surface (Fig. 1). Endocytosis vesicles were rare finding. Large nucleus of oval or beanlike shape had high content of euchromatin and prominent well-structured nucleoli with large granular zone. Volume of cytoplasm and number of cell organelles varied in different cells depending on their sizes. Cytoplasm had average electron density, grainy structure and few cisterns of rough endoplasmic reticulum. Short oval mitochondria (about 0.5  $\mu$ m in length) having matrix of average electron density and rare cristae were accumulated near the nucleus. The Golgi complex was small, sparse "coated" and smooth-membrane vesicles were seen around short flattened cisterns showing low activity of intracellular membrane transport. Multivesicular bodies and lysosomes were extremely rare in tumor RLS cells. Many large cells contained relatively big lipid droplets (Fig. 1, b). In general, cells of tumor RLS in ascitic fluid showed poor signs of membrane-associated synthesis and transport against active production of ribosomes in large nucleoli. Probably the metabolism in ascitic tumor cells mainly occurred in non-membrane compartments.

Histological examination of kidneys in mice inoculated with tumor RLS found metastasis foci in pelvis area and in cortex (Fig. 2, a, b), while in kidney medulla the metastases were not detected during whole experiment. The observed distribution of metastases corresponded with location of lymphosarcoma metastases in kidneys of sick humans [6, 15]. Metastasizing lymphosarcoma cells spread mainly by hematogenic way [16], so absence of metastases in kidney medulla is probably related to low blood flow in this part of the organ.

The kidneys of mice on day 8 after inoculation of the tumor RLS showed 6–8 metastases (40–60  $\mu$ m in size) in kidney cortex per sagittal section. Number of metastases in renal pelvis area was 4–6 metastases

per section. Sizes of these metastases varied from 50 to 100  $\mu\text{m}$  after 14 days post inoculation of the tumor RLS. All the metastases comprised of identical cells having size 4–6  $\mu\text{m}$ . These cells had roundish nucleus edged by small ring of weakly basophilic cytoplasm (Fig. 2, *a, b*). The reaction with antibodies for Ki-67 protein was negative showing arrest of mitotic division of tumor cells. Reaction for Apaf-1 protein also was negative, indicating the absence of apoptosis.

The morphology of metastases in kidney cortex and in renal pelvis area changed after two series of PCT injections (15 days post inoculation of the tumor). In kidney cortex number of metastases consisting of small cells decreased, and their size diminished to 20–50  $\mu\text{m}$ . Size of metastases in renal pelvis area also decreased (to 50–70  $\mu\text{m}$ ), number of cell elements lessened, and they were separated by layers of connective tissue. Metastases located in renal pelvis area contained cells positively stained for anti-Apaf-1 protein that indicate apoptosis (Fig. 2, *c*). Reaction with antibodies for Ki-67 protein was negative in all of the metastases that point to suppression of tumor RLS cells proliferation. At the same time with regression of small cell metastases we found large tumor cells of 12–18  $\mu\text{m}$  in size (some of them exceed 30  $\mu\text{m}$ ) in kidney parenchyma. On paraffin sections these cells had dark polymorphous nucleus with barely discernible borders and huge homogeneous basophilic cytoplasm (Fig. 2, *d*).

Next time point of the experiment, 21 days post inoculation of the tumor RLS, showed absence of small cell metastases in mice kidneys, instead of them large cell metastases of 50–80  $\mu\text{m}$  size were observed in kidney cortex. “Explosive” growth of metastases in kidney cortex was observed in period of days 22–29 after tumor RLS inoculation (3 and 4 series of PCT injections): their number was 16–22 per sagittal section and size was 30–130  $\mu\text{m}$  (Fig. 2, *e*). The metastases in this period consisted only of large cells, which demonstrated proliferative activity (positive reaction with anti-Ki-67 antibodies) despite injections of cytostatics. No signs of apoptosis were observed.

Electron-microscopic study of large tumor RLS cells revealed polymorphous nuclei with matrix of average density, small clumps of heterochromatin and prominent large nucleolus (Fig. 2 *e, f*). The cells contained grainy cytoplasm, long cisterns of rough endoplasmic reticulum, numerous free ribosomes, well-developed cisterns of Golgi complex, multivesicular bodies, electron dense lipid droplets, “coated” vesicles. Number of mitochondria varied from a few to some tens per cell section. The structure of large cells in kidney metastases indicated active metabolic processes both in membrane- and non-membrane compartments.

Thus, injections of cytostatic preparations under the scheme CHOP to mice resulted in disappearance of metastases consisting of small (4–5  $\mu\text{m}$ ) cells and development of metastases formed by large tumor cells (12–18  $\mu\text{m}$ ). Earlier studies showed that a suspension of cells of ascitic tumor RLS contained 10% cells with MDR phenotype [10], thereby we inoculated mice with a mixture of 90% sensitive to PCT cells, and 10% — resistant. We propose that large cells which appeared in kidneys during the PCT and formed metastases represent a progeny of MDR phenotype cells injected in mice. Apparently PCT serves as selective factor for these cells which can proliferate in tumor node and then migrate to kidneys. Presence of proliferative activity in large-cell metastases illustrates their resistance to PCT. In this way tumor RLS has heterogeneous cellular structure and contains at least two kinds of cells. Presence of large tumor cells, which preserve ability to proliferate and metastasize during PCT, supports the concept of “stem” tumor cells, existence of which was shown in glioblastoma, benign papilloma and intestinal adenoma [17–19].

Histological structure of the kidneys in intact CBA mice corresponded to those described for this animal species [20, 21]. Light microscopy of kidneys on day 8 after tumor RLS inoculation in mice revealed pathological changes which were not directly related with metastases. The tissues neighboring with the metastases maintained their “normal” histological structure. The injury was

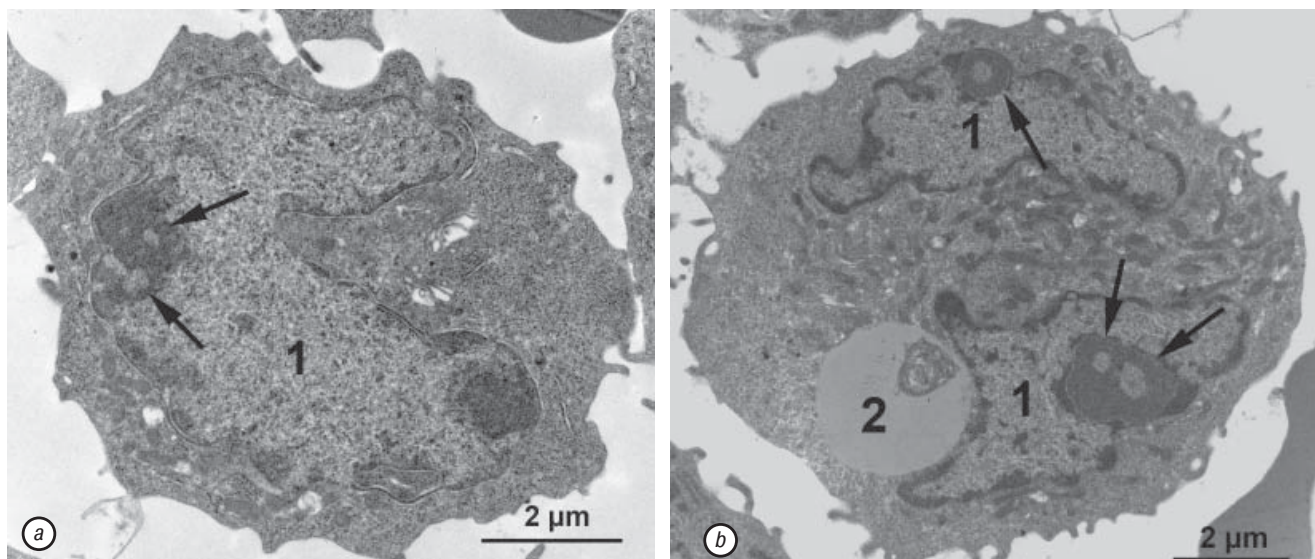


**Fig. 1.** Small (*a*) and large (*b*) cells of tumor RLS in ascities fluid of CBA mice. 1 — nucleus, 2 — lipid droplet, arrows show the nucleoli. Ultrathin sections, transmission electron microscopy (x 40000)

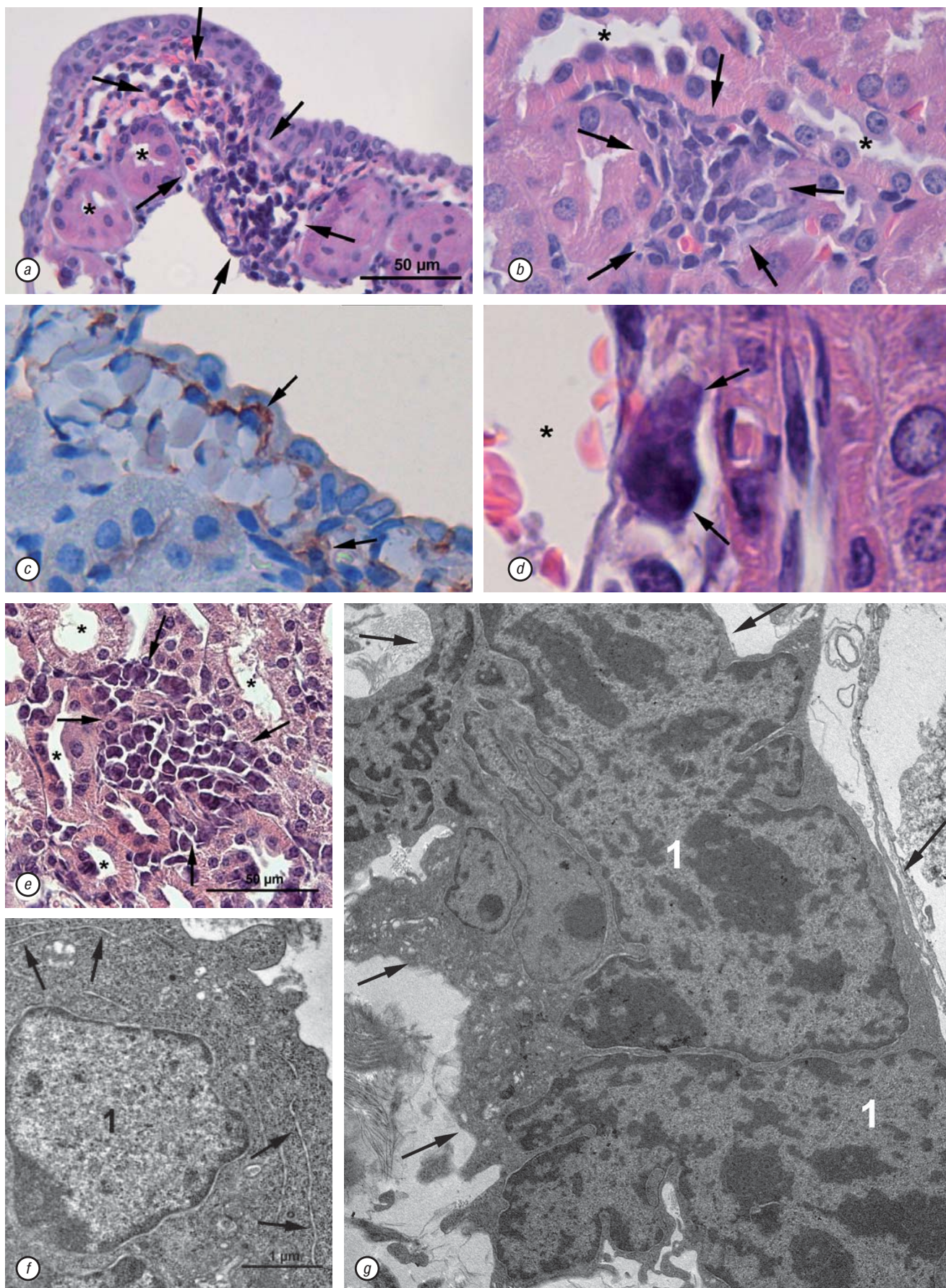


**Fig. 2.** Metastases (shown with arrows) of tumor RLS in renal pelvis area (HE $\times$ 40) (a) and kidney cortex (HE $\times$ 100) (b) of mice received PCT under scheme CHOP, 8 days after tumor inoculation (1 series of PCT injections). Asterisks show kidney tubules. Positive reaction with anti-Apaf-1 antibodies (shown by arrows) in pelvis area (x40) (c) of a mouse, 21 days post inoculation of the tumor RLS, 2 series of PCT injections. Large tumor cell (shown by arrows) in kidney tissue (HE $\times$ 100) (d), 15 days post inoculation of the tumor, 2 series of PCT injections; asterisk indicates lumen of blood vessel. Metastasis (shown by arrows) in kidney cortex (HE $\times$ 40) (e) 28 days after tumor inoculation, 3 series of PCT injections; asterisks show kidney tubules. Large tumor cells in mice kidney (f, g), 28 days after tumor inoculation, 3 series of PCT injections. 1 — nucleus, 2 — nucleolus, arrows show endoplasmic reticulum on fig. f, and cell borders — on fig. g. Ultrathin sections, transmission electron microscopy (x 50000, x 15000)

observed in proximal tubules of outer strip, where S3-segments of the tubules are located, and involved about 5% of area in kidney sections. Proximal tubules showed widening of lumen and cell debris in the lumens; some foci composed of necrotic epitheliocytes and epitheliocytes with homogeneous bright eosinophilic cytoplasm (2–3 cells in field of view at a 400x magnification) also were observed (Fig. 3, a). Eosinophilic cells showed high electron density of cytoplasm and hardly discerned organoids in ultrathin sections. Similar eosinophilic cells in proximal tubules of rodents were described in different studies and are considered as a sign of necrotic changes of the epitheliocytes [22, 23].

Electron microscopy found decrease of cytoplasm density in proximal tubule cells in area of outer strip after a day post first injections of PCT preparations; many of the cells showed visible reduction of folds in basal plasmalemma, while number of apical microvilli visually did not change (Fig. 3, b). Alteration of plasmalemma organization indicates the impairment of ion transport and perhaps is related with overlapping impacts of tumor process and cytostatic preparations, particularly cyclophosphamide. Cyclophosphamide and its metabolites cause dose-dependent rise of expression of aquaporines 1 and 7 (AQP1 and AQP7) in kidney tubules of rodents and thereby disturb water-ion transport. It is interesting that expression of AQP7 reveals itself only in cells of S3-segment of proximal tubules [24, 25]. Another factor of alteration of the cells of S3-segment by various anti-tumor preparations is high activity of glutathion-synthase [26]. Thus, selective alteration of cells in S3-segment of mice kidney found in this study corresponds to known higher sensitivity of the S3-segments to damaging factors in comparison with other parts of nephron [24].

Toxic effect of PCT also touched mitochondria of epithelium in proximal tubules which changed their shape to roundish. Similar change of mitochondria shape was reported after injections of cisplatin, which has nephrotoxic effect [27]. Thereby, single application of preparations under scheme CHOP caused distinct damage to epithelium of proximal tubules and first of all to cells of S3-segment in RLS-bearing mice. First injection of PCT preparations also affected interstitial tissue of kidneys which showed prominent changes: swelling of collagen fibers and break of their characteristic striation, increase of electron density of intercellular matrix (Fig. 3, c). These changes were present in kidney cortex during whole experiment and were observed in all mice treated with PCT.

Morphology of renal bodies looked unaltered in this period, some of the bodies showed widening of filtration space in comparison with that in non-damaged areas (7.26 and 2.1  $\mu\text{m}$  correspondingly) what points to malfunction of primary urine outflow. Morphology of medulla and distal tubules did not visually differ from those in intact mice.

After second injection of PCT preparations (15<sup>th</sup> day post inoculation of the tumor) pathologically changed area of kidney cortex grew, as well as number and area of necroses in proximal tubules. “Sludge” of eryth-

rocytes and change of blood plasma which became electron dense were observed in blood vessels of kidneys signaling about alteration of organ blood supply. Morphology of other structures of kidney remained visually unchanged. Ultrastructural examination of kidneys showed disappearance of basal folds of plasmalemma in cells of proximal tubules in all mice, indicating a break of cell functions. Basal folds normally occupy large areas in proximal tubule cells providing essential square for water-ion transport. How can they disappear? We found myelin-like structures which looked similar to a ball of string on the cut in these cells (Fig. 3, d). We suppose that these structures represent final stage of basal folds degradation. Basal folds altered by cytostatics would be internalized by cells for further destruction and new portions of membrane components would be inserted into basal plasmalemma. Absence of signs of plasmalemma “recovery” represents another evidence of dramatic alteration of epithelial cells in proximal tubules in mice received PCT. The disappearance of basal folds in epithelium of proximal tubules under the PCT or single cytostatics influence was not reported yet.

Pathologic changes in nephrons grew a week after 3<sup>rd</sup> injection of PCT preparations (28<sup>th</sup> day after tumor inoculation) and involved distal and proximal tubules in kidney cortex. Epithelial cells of distal tubules showed decreased electron density of cytoplasm and electron-dense lipid droplets (Fig. 3, e). Epitheliocytes of proximal tubules contained myelin-like structures in cytoplasm and no basal folds. These cells significantly decreased in the height, number of apical microvilli markedly reduced, and electron-dense lipid droplets accumulated in cytoplasm (Fig. 3, b). Similar changes were described in kidneys of rats injected with doxorubicin [28, 29].

Pathological changes in kidneys increased after four series of injections of PCT preparations (29<sup>th</sup> day post inoculation of the tumor). Lesion of proximal tubules extended to about 50% of kidney section, necroses spread to considerable part of kidney cortex. Small cavities appeared in kidney interstitial tissue looking similar to those described in rodents after single injection of doxorubicin [28, 29]. It should be noted that development of pathological changes of epithelium in distal tubules “falls behind” the damage of proximal tubules. We observed widening of filtration space and lumens of capillaries in renal bodies (Fig. 3, f), some capillaries contained clumps of electron dense plasma and cell detritus. Widening of capillary lumen can be a consequence of malfunction of blood supply and of toxic impact of doxorubicin upon endothelial functions [30].

In contrast to tubular epithelium, podocytes remained unaltered against the background of PCT, however signs of activation of synthetic processes in these cells were observed. Increase of number of granular endoplasmic reticulum cisterns and length of cisterns of Golgi complex was seen in these cells. Number of “coated” vesicles and multivesicular bodies grew showing activation of clathrin-dependent endocytosis. Similar changes in kidneys of mice were caused by single injection of doxorubicin [29]. So, podocytes possess relative resistance to impact

of chemotherapeutic drugs, which caused activation of metabolic processes in these cells.

Our study was the first attempt to visualize and describe changes which develop in kidneys during

PCT treatment of lymphosarcoma. Toxic impact of PCT is well known [1, 2], and we tried to trace development of pathological changes caused by PCT in mice bearing the tumor RLS. The obtained results showed that

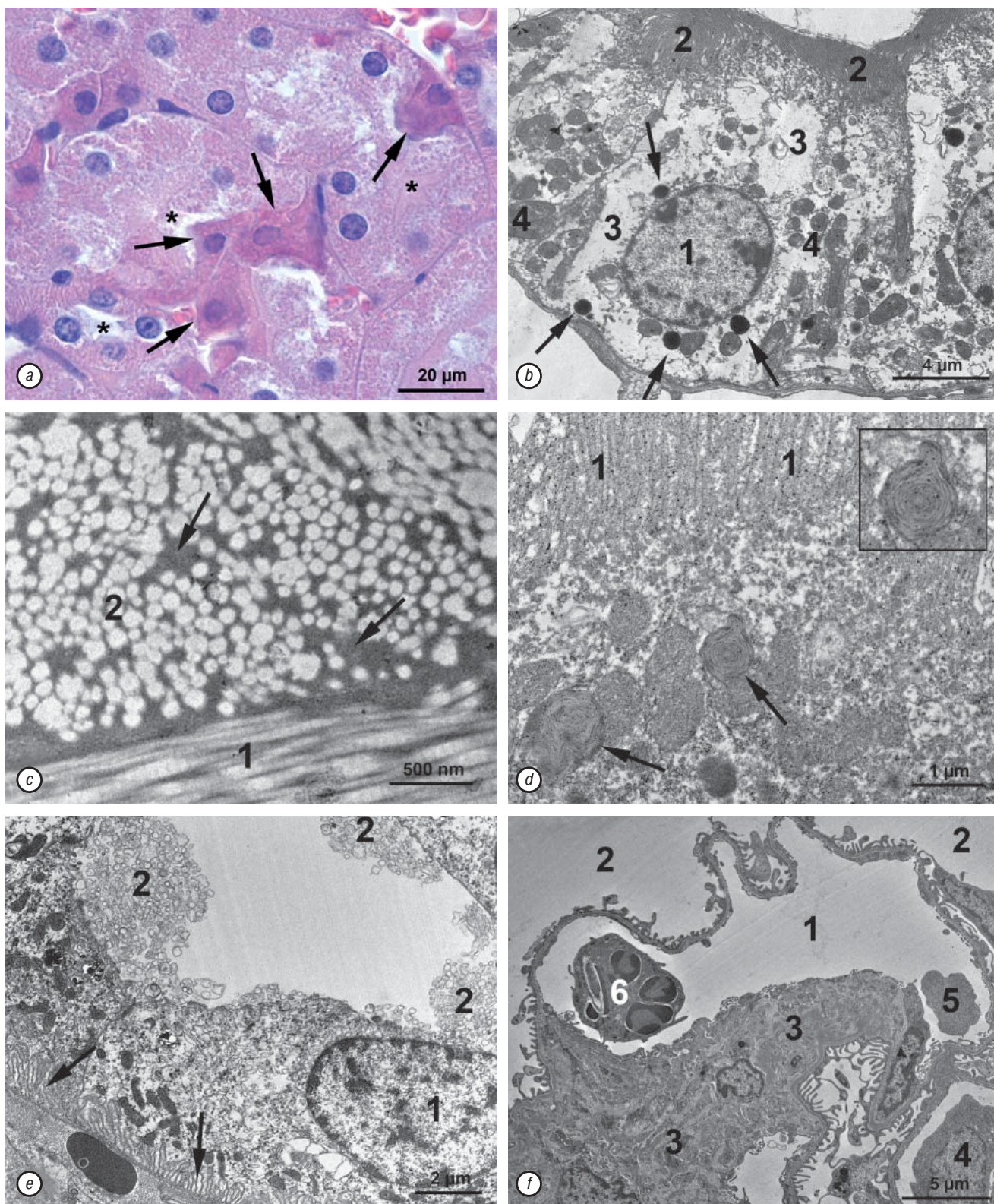


**Fig. 3.** Outer strip area of kidney (HEX100) (a) in a mouse received PCT under scheme CHOP, 8 days after tumor RLS inoculation (1 series of PCT injections). Arrows show bright eosinophilic cells, asterisks show lumen of kidney tubules. Cells of proximal tubule (x20000) (b), 28 days after tumor RLS inoculation, 3 series of PCT injections. 1 — nucleus, 2 — microvilli, 3 — cytoplasm, 4 — roundish mitochondria, arrows show electron-dense lipid droplets. Longitudinal (1) and transverse (2) sections of collagen fibers in interstitial tissue of mouse kidney (x100000) (c), 8 days after tumor RLS inoculation, 1 series of PCT injections. Arrows show electron-dense intercellular matrix. Apical area of proximal tubule cell (x80000) (d), 21 days after tumor inoculation, 2 series of PCT injections. 1 — microvilli, arrows and box show myelin-like structures. Cells of distal tubule (x30000) (e), 21 days after tumor RLS inoculation, 2 series of PCT injections. 1 — nucleus, 2 — cell debris in tubule's lumen, arrows show basal folders of plasma membrane. Kidney glomeruli (x15000) (f), 28 days after tumor RLS inoculation, 3 series of PCT injections. 1 — widened capillary, 2 — filtration space, 3 — mesangial tissue, 4 — nucleus of podocyte, 5 — cell debris, 6 — neutrophil. Ultrathin sections, transmission electron microscopy

PCT leads to prominent structural damage of nephron cells, primarily in proximal tubules, which are responsible for transport of water, ions, metabolites and xenobiotics through epithelial barrier. Electron microscopy demonstrated that PCT impact was primarily directed to plasmalemma and mitochondria — the structures responsible for water-ion transport. Pathological changes found in mice obviously reflect mechanisms of PCT toxic impact and should be considered while designing of remedies for recovery of visceral organs after PCT of oncologic diseases.

### ACKNOWLEDGEMENTS

This work was supported by a grant from “OPTEC” (Russia) company.

### REFERENCES

1. Sanderson H, Brain RA, Johnson DJ, *et al.* Toxicity classification and evaluation of four pharmaceuticals classes: antibiotics, antineoplastics, cardiovascular, and sex hormones. *Toxicology* 2004; **203**: 27–40.
2. Fisher RI, Gaynor ER, Dahlborg S, *et al.* Comparison of a standard regimen (CHOP) with three intensive chemotherapy regimens for advanced non-Hodgkin's lymphoma. *New Engl J Med* 1993; **328**: 1002–6.
3. Richmond J, Sherman RS, Diamond HD, *et al.* Renal lesions associated with malignant lymphomas. *Am J Med* 1962; **32**: 184–207.
4. Senkova AV, Ageeva TA, Zenkova MA. Mutual relation of processes of progressing of plural medicinal resistance in the tumour and morphological changes in the liver at mice with interwind lymphosarcoma RLS40 in the conditions of polychemotherapy. *SB RAMS Bulletin* 2011; **31**: 87–93.
5. Jhamp R, Gupta N, Garg S, *et al.* Diffuse lymphomatous infiltration of kidney presenting as renal tubular acidosis and hypokalemic paralysis case report. *Croat Med J* 2007; **6**: 860–3.
6. Moslemi MK, Tahvildar SA, Ashtari A. Primary lymphoma of the kidney in an adult male — the first reported case from Iran. *Case Rep Oncol* 2010; **3**: 72–6.
7. Andreeva EM, Mironova EL, Shklyayeva OA, *et al.* Implication *mdr1a*, *mdr1b*, *p53* and *bcl-2* genes in resistance of mice lymphosarcoma RLS to therapeutic effect of cyclophosphamide. *NSU messenger* 2006; **4**: 21–6.
8. Melnikova EV, Grishanova AY, Kaledin VI, *et al.* Ceramide accumulation disturbance in transplantable cyclophosphamide-resistant lymphosarcoma of mice. *SB RAMS Bulletin* 2008; **6**: 14–6.
9. Simon SM, Schindler M. Cell biological mechanisms of multidrug resistance in tumors. *Proc Natl Acad Sci* 1994; **91**: 3497–504.
10. Mironova N, Shklyayeva O, Andreeva E, *et al.* Animal model of drug-resistant tumor progression. *Ann NY Acad Sci* 2006; **1091**: 490–500.
11. Kaledin VI, Nikolin VP, Ageeva TA. Cyclophosphamide-induced apoptosis in mice lymphosarcoma cells *in vivo*. *Onc Questions* 2000; **46**: 588–93.
12. Gerdes J, Lemke H, Baisch H, *et al.* Cell cycle analysis of a cell proliferation-associated human nuclear antigen defined by the monoclonal antibody Ki-67. *J Immunol* 1984; **4**: 1710–5.
13. Braun N, Paradopoulos T, Muller-Hermelink HK. Cell cycle dependent distribution of the proliferation-associated Ki-67 antigen in human embryonic lung cells. *Virch Arch B Cell Pathol Incl Mol Pathol* 1988; **1**: 25–33.
14. Cohen LJ, Rennke HG, Laubach JP, *et al.* The spectrum of kidney involvement in lymphoma: a case report and review of the literature. *Am J Kidney Diseases* 2010; **6**: 1191–6.
15. Morel P, Dupriez B, Herbrecht R, *et al.* Aggressive lymphomas with renal involvement: a study of 48 patients treated with the LNH-84 and LNH-87 regimens. *Br J Cancer* 1994; **70**: 154–9.
16. Jafri SZH, Bree RL, Amendola MA, *et al.* CT of renal and perirenal non-Hodgkin lymphoma. *AJR* 1982; **138**: 1101–5.
17. Chen J, Li Y, Yu TS, *et al.* A restricted cell population propagates glioblastoma growth after chemotherapy. *Nature* 2012; **488**: 522–6.
18. Driessens G, Beck B, Caauwe A, *et al.* Defining the mode of tumour growth by clonal analysis. *Nature* 2012; **488**: 527–30.
19. Schepers AG, Snippert HJ, Stange DE, *et al.* Lineage tracing reveals Lgr5+ stem cell activity in mouse intestinal adenomas. *Science* 2012; **337**: 730–5.
20. Bulger RE, Doby DC. Recent advances in renal morphology. *Annu Rev Physiol* 1982; **44**: 147–79.
21. Michael AF, Keane WF, Raji L, *et al.* The glomerular mesangium. *Kidney Int* 1980; **17**: 141–54.
22. Lee HT, Park SW, Kim M, *et al.* Acute kidney injury after hepatic ischemia and reperfusion injury in mice. *Lab Invest* 2009; **89**: 196–208.
23. Leventhal JS, Alsauskas Z, Snyder A, *et al.* Renal HIV expression is unaffected by serum LPS levels in an HIV transgenic mouse model of LPS induced kidney injury. *PLoS One* 2011; **6**.
24. Kim S, Jo CH, Park J, *et al.* The role of proximal nephron in cyclophosphamide-induced water retention: preliminary data. *Electrolyte Blood Press* 2011; **9**: 7–15.
25. Sekine M, Monkawa T, Morizane R, *et al.* Selective depletion of mouse kidney proximal straight tubule cells causes acute kidney injury. *Transgenic Res* 2011; **21**: 51–62.
26. Cristofori P, Zanetti E, Fregona D, *et al.* Renal proximal tubule segment-specific nephrotoxicity: an overview on biomarkers and histopathology. *Toxicol Pathol* 2007; **35**: 270–5.
27. Brooks C, Wei Q, Cho S, *et al.* Regulation of mitochondrial dynamics in acute kidney injury in cell culture and rodent models. *J Clin Invest* 2009; **119**: 1275–85.
28. Wang Y, Wang PY, Tay Y, *et al.* Progressive adriamycin nephropathy in mice: Sequence of histologic and immunohistochemical events. *Kidney Int* 2000; **58**: 1797–804.
29. Ayla S, Seckin I, Tanriverdi G, *et al.* Doxorubicin induced nephrotoxicity: Protective effect of nicotinamide. *Int J Cell Biol* 2011; **2011**: 1–9.
30. Jeansson M, Bjorck K, Tenstad O, *et al.* Adriamycin alters glomerular endothelium to induce proteinuria. *J Am Soc Nephrol* 2009; **20**: 114–22.